Minimum entropy production in a distillation column for air separation described by a continuous non-equilibrium model

Diego Kingston[a,d,*], Øivind Wilhelmsen[b,c], Signe Kjelstrup[d]

[a] *Universidad de Buenos Aires, Facultad de Ingeniería, Departamento de Química, Paseo Colón 850, C1063ACV, Buenos Aires, Argentina*
[b] *Department of Energy and Process Engineering, Norwegian University of Science and Technology, NO-7491, Trondheim, Norway*
[c] *SINTEF Energy Research, NO-7465, Trondheim, Norway*
[d] *PoreLab, Department of Chemistry, Norwegian University of Science and Technology, NO-7491, Trondheim, Norway*

Abstract

In this work, we apply the rate-based model of Taylor and Krishna to describe the separation of air in a low-pressure, packed distillation column. By use of numerical optimization, we identify the temperature profile for heat exchange with the column and its surroundings that minimizes the total entropy production. Optimal operation of the column reduces the entropy production by nearly 50 %, and the total heating- and cooling duties by 30 % and 50 %, respectively. We find that the local entropy production is more uniform for the optimal solution than in the adiabatic column, a property that may be helpful for new designs. Using the equilibrium stage model, the state of minimum entropy production has higher cooling/heating duties than in the rate-based model case. This shows that more sophisticated models can be beneficial for the development of reliable strategies, to improve the energy efficiency of distillation columns.

Keywords: diabatic distillation, entropy production, Non-Equilibrium Thermodynamics, air separation

Nomenclature

Latin symbols

a	Surface area between liquid and vapor per unit volume of packing	$(\mathrm{m}^2 \cdot \mathrm{m}^{-3})$
a^H	Heat exchange area with utility per unit volume of packing	$(\mathrm{m}^2 \cdot \mathrm{m}^{-3})$
A	Exchange area between liquid and vapor	(m^2)
A^H	Tray heat exchange area with utility	(m^2)
B	Bottoms molar flow	$(\mathrm{mol} \cdot \mathrm{s}^{-1})$
c_p	Molar heat capacity	$(\mathrm{J} \cdot \mathrm{mol}^{-1} \cdot \mathrm{K}^{-1})$
c_t	Molar density	$(\mathrm{mol} \cdot \mathrm{m}^{-3})$
D	Distillate molar flow	$(\mathrm{mol} \cdot \mathrm{s}^{-1})$
dS^{irr}/dt	Total entropy production	$(\mathrm{W} \cdot \mathrm{K}^{-1})$
F	Total feed molar flow	$(\mathrm{mol} \cdot \mathrm{s}^{-1})$
h	Molar enthalpy	$(\mathrm{J} \cdot \mathrm{mol}^{-1})$
$\bar{h}_k$	Partial molar enthalpy of component k	$(\mathrm{J} \cdot \mathrm{mol}^{-1})$
J_e	Total energy flux	$(\mathrm{W} \cdot \mathrm{m}^{-2})$
J_k	Component molar flux	$(\mathrm{mol} \cdot \mathrm{m}^{-2} \cdot \mathrm{s}^{-1})$
J_q	Heat flux within the utility	$(\mathrm{W} \cdot \mathrm{m}^{-2})$
J'_q	Measurable heat flux	$(\mathrm{W} \cdot \mathrm{m}^{-2})$
k	Mass transfer coefficient	$(\mathrm{m} \cdot \mathrm{s}^{-1})$

*Corresponding author
Email address: dkingston@fi.uba.ar (Diego Kingston)

This is the accepted version of an article published in Chemical Engineering Science
http://dx.doi.org/doi.org/10.1016/j.ces.2020.115539

K_j	Thermodynamic K-factor of component j	$(-)$
ℓ_R	Height of packing in the rectification section	(m)
ℓ_S	Height of packing in the stripping section	(m)
L	Total liquid molar flow	$\left(\mathrm{mol}\cdot\mathrm{s}^{-1}\right)$
L_k	Component molar flow in liquid	$\left(\mathrm{mol}\cdot\mathrm{s}^{-1}\right)$
$\dot{Q}$	Heat flow	(kW)
r	Reflux ratio	$(-)$
R	Universal gas constant	$\left(\mathrm{J}\cdot\mathrm{mol}^{-1}\cdot\mathrm{K}^{-1}\right)$
s	Molar entropy	$\left(\mathrm{J}\cdot\mathrm{mol}^{-1}\cdot\mathrm{K}^{-1}\right)$
T	Temperature	(K)
T_B	Bubble temperature	(K)
T_D	Dew temperature	(K)
U	Overall heat transfer coefficient with utility	$\left(\mathrm{W}\cdot\mathrm{m}^{-2}\cdot\mathrm{K}^{-1}\right)$
V	Total vapor molar flow	$\left(\mathrm{mol}\cdot\mathrm{s}^{-1}\right)$
V_k	Component molar flow in vapor	$\left(\mathrm{mol}\cdot\mathrm{s}^{-1}\right)$
x_k	Component molar fraction in liquid	$(-)$
X_k	Thermodynamic driving force for mass transfer	$\left(\mathrm{J}\cdot\mathrm{mol}^{-1}\cdot\mathrm{K}^{-1}\right)$
X_q	Thermodynamic driving force for heat transfer	$\left(\mathrm{K}^{-1}\right)$
y_k	Component molar fraction in vapor	$(-)$
z	Position along the axis of the column	(m)

Greek symbols

β	Ratio a^H/a	$(-)$
Δ	Difference	$(-)$
$\Delta\mu_{k,T}$	Chemical potential difference evaluated at a constant temperature	$\left(\mathrm{J}\cdot\mathrm{mol}^{-1}\right)$
Λ	Heat transfer coefficient	$\left(\mathrm{W}\cdot\mathrm{m}^{-2}\cdot\mathrm{K}^{-1}\right)$
σ	Local entropy production per area	$\left(\mathrm{W}\cdot\mathrm{m}^{-2}\cdot\mathrm{K}^{-1}\right)$
ϕ	Vapor fraction	$(-)$
$\hat{\phi}_k$	Fugacity coefficient of component	$(-)$
Ω	Cross sectional area	$\left(\mathrm{m}^2\right)$

Superscripts and subscripts

∞	Utility
B	Bottoms
C	Condenser
D	Distillate
F	Feed
I	Interface
V	Vapor phase
L	Liquid phase
LV	Difference between liquid and vapor
LU	Difference between liquid and utility
R	Reboiler
RS	Rectification section
S	Section
SS	Stripping section

1. Introduction

Distillation is among the separation processes that are most widely used in the chemical industry [31]. In order to separate components of different volality, energy is added at the bottom of the column (the reboiler) and removed at the top (the condenser). This makes distillation an energy intensive operation [27], and has motivated numerous studies to increase the energy efficiency. One of the major drawbacks of distillation is the exergy losses associated with the temperature difference between the heat source and sink, leading to an overall low thermodynamic efficiency [12].

Conventional distillation columns are usually adiabatic; heat can only be exchanged in the reboiler and condenser. One way to improve their efficiencies is to allow for heat exchange with the column, making

This is the accepted version of an article published in Chemical Engineering Science
http://dx.doi.org/doi.org/10.1016/j.ces.2020.115539

it diabatic [19, 11, 22]. By gradually supplying and removing heat along the rectification and stripping sections, it is possible to use the heats of condensation and evaporation more efficiently. This is because such heat exchange takes place at smaller temperature differences, reducing the thermal exergy destruction [12].

The energy efficiency, lost work and exergy destruction of distillation columns are linked to the total entropy production via the Gouy-Stodola theorem, see *e.g.* [13]. Since the entropy production is the true source of irreversibilities, minimization of the entropy production in diabatic distillation columns has attracted considerable interest in the literature [5, 11, 22, 23, 24, 25, 26]. Previous studies have shown that the potential to improve the energy efficiency is large. For example, Røsjorde and Kjelstrup [22] showed that the savings of a typical propane/propylene splitting unit could be in the order of 1 to 2 GWh per year. Sauar et al. [24] found that for the benzene-toluene column alone, the entropy production could be reduced by 37.3 % with proper thermal management. More recent work by de Koeijer et al. [5] indicated that the entropy production could be decreased by as much as 80 % for the same mixture. All these studies were conducted with the so-called equilibrium stage-model for distillation; assuming separation in stages, with equilibrium of liquid and vapor at the outlet of each stage. One aim of the present work is to relax this assumption and replace the it by the well established rate-based model of Taylor and Krishna [29]. Also, utilities were earlier taken into account to a varying degree. In this work, we include a full set of auxiliary equipments for heat exchange in the analysis of the total process.

In the early studies, different criteria and methods were used to identify or approximate the state of minimum entropy production. Sauar et al. [24] for example, arrived at the concept called "equipartition of driving forces". They did not invoke the energy balance in their derivation of this concept, however. Schaller et al. [25, 26] found that the stages of the optimal column should all be characterized by "equal thermodynamic distance". This was in agreement with numerical optimization studies of columns with a large number of trays. According to optimal control theory, a more general guideline for optimal operation is "equipartition of entropy production" (EoEP) [13, 30]. This was applied to the optimization of distillation columns, mostly in combination with the equilibrium stage model [11, 5, 14, 23]. De Koeijer et al. [5] and Sauar et al. [24] compared these criteria to the outcome from numerical algorithms. Although the optimal operating conditions according to each concept differed from one another, the entropy production was similar. This indicates that the minimum was rather flat [5, 24].

The works reviewed above have all found the optimal heating- and cooling profiles along the column and the optimal allocation of a fixed total transfer area through the column that characterize minimum entropy production. However, little attention was paid to the total heating and cooling duties, which are important performance indicators. Exceptions are Refs. [11, 22, 24] where the trade-off between lower entropy production and higher heating/cooling duties is discussed. Nevertheless, the experimental results of de Koeijer and Rivero [3] showed for similar separation requirement, that the duty of a diabatic column was smaller than that of an adiabatic column.

This may indicate that unrealistic simplifications have been imposed in previous works. Therefore, in addition to removing the assumption of equilibrium between vapor and liquid through the column, we shall include in the analysis the reboiler and condenser.

We shall use as example the cryogenic separation of air, as this is a central, important and mature process [1]. The efficiency of the cryogenic air separation process has been studied by exergy analysis in previous works [1]. The integration of parts of a higher pressure rectification and a lower pressure stripping sections via heat exchangers was studied, leading to a reduction of exergy losses by 8.5 %. Van der Ham [32] studied the exergy efficiency of a cryogenic air separation unit as part of an integrated gasification combined cycle. Fu and Gundersen [6] used exergy analysis to reduce power consumption in air separation units for oxy-combustion processes. They indicated that the power consumption was about 4.7 times the theoretical minimum. However, significant improvements could not be expected before the flowsheet structure is modified. Zhou et al. [37] proposed a near-atmospheric column with a thermal pump as an alternative to the conventional double column, performing energy- and exergy analyses. They estimated that the energy consumption could be reduced by 23 %, while the exergy efficiency could be increased by 2 to 6 %. In this work, we shall reveal an even larger potential to improve the distillation column.

The construction and operation of distillation columns require large investments. This has motivated

This is the accepted version of an article published in Chemical Engineering Science
http://dx.doi.org/doi.org/10.1016/j.ces.2020.115539

the development of mathematical models of different complexity [31]. They are broadly classified into two groups: equilibrium-stage and rate-based (or non-equilibrium) models [27, 29]. It is the first category that relies on the assumption that the vapor and liquid leaving each stage are in equilibrium with one another. Hence, only information about equilibrium properties and solution of global mass and energy balances is required when this model is used [27]. In contrast, the rate-based models use transport equations for heat and mass transfer, as well as separate balance equations for the vapor and liquid phases [27, 29]. Even though the equilibrium-stage model has been widely used for simulation of distillation columns, it has long been recognized that non-equilibrium models are more reliable [15, 29]. It is possible to account for deviations from equilibrium by incorporating, for example, a Murphree efficiency [27]. However, the Murphee efficiency has met criticism in the literature, specially in the case of multicomponent systems [29]. We have therefore opted for the alternative to use the full rate-based model.

Rizk et al. [20] used a non-equilibrium model to simulate a packed cryogenic air separation unit and performed an exergy analysis of a heat integrated column. They showed that its exergy efficiency is 23 % higher than that of a conventional column. Their model had some limitations, e.g., that the rates of nitrogen and oxygen transfer had a fixed ratio, given by the heats of vaporization. Also, they only considered diffusive transport. Chang and Liu [2] used a more rigorous non-equilibrium model for a heat -integrated stage column for separation of nitrogen, oxygen and argon. They showed that the Murphree efficiencies were below 0.7 and had different values for the components. Takamatsu et al. [28] used a rate-based model to simulate a heat-integrated distillation column (HIDiC) for a binary mixture of water and methanol. They showed that such a configuration lead to 30 % reduction in the energy supply in comparison to a conventional column operating at minimum reflux. We shall see that the state of minimum entropy production for rate-based column models differs qualitatively from the corresponding state of an equilibrium-stage model. Also, the use of the rate-based model allows us to compare results to those predicted by EoEP [10].

The work is organized as follows. Section 2 presents the governing equations and assumptions. In Sec. 3, we give details about the numerical methods used to solve the column model as well as the optimization routine. Results are discussed in Sec. 4 and concluding remarks are provided in Sec. 5.

2. Model for the distillation column

We present a model for a continuous (packed) distillation column for the separation of a binary mixture of nitrogen-(1) and oxygen-(2), following the works of Johannessen [8] and Taylor and Krishna [29]. This includes a total condenser and a partial reboiler. A sketch of the column is presented in Fig. 1. The model relies on the following assumptions:

1. The column operates at steady-state.
2. The components' mole fractions, velocity and temperature of each phase are uniform in a cross-section.
3. There is no entrainment of liquid in the vapor phase, nor is there vapor trapped in the liquid.
4. There is equilibrium at the interface.
5. There is no back-mixing in the column.
6. The pressure drop across the section and auxiliary equipment (reboiler and condenser) is negligible.
7. The reboiler behaves as an ideal equilibrium-stage.
8. When the column is operated in a diabatic way, heat exchange takes place between the utility and liquid.

This is the accepted version of an article published in Chemical Engineering Science
http://dx.doi.org/doi.org/10.1016/j.ces.2020.115539

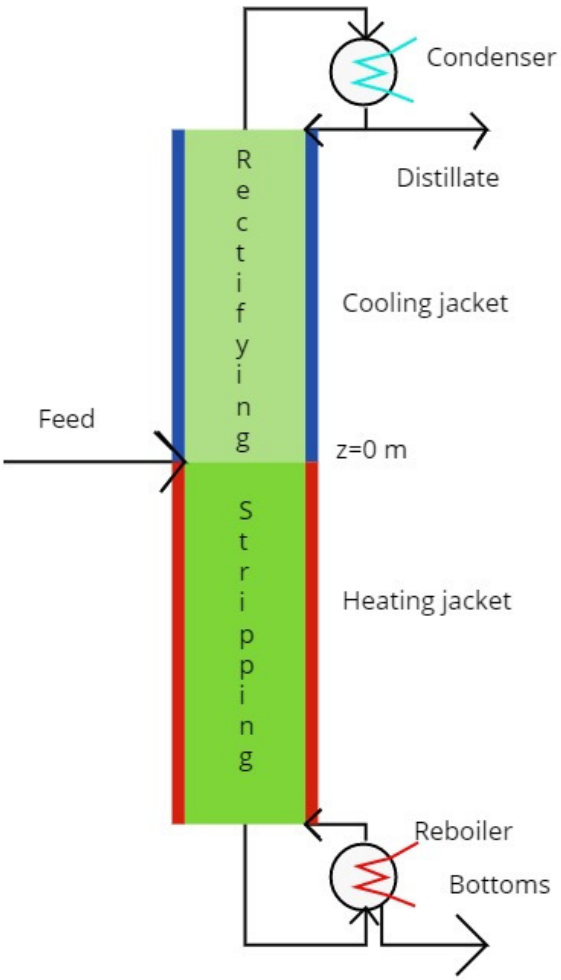

Figure 1: An illustration of the system modeled. In the optimization procedure, a utility at temperature $T_\infty(z)$ interacts with the rectifying and stripping section at every vertical position, z. $z = 0$ is defined to be where the feed enters.

2.1. Balance equations for the column

The governing equations for the rectification and stripping sections were given by Johannessen [8],

$$\frac{dV_k}{dz} = J_k a\Omega, \tag{1}$$

$$\frac{dL_k}{dz} = J_k a\Omega, \tag{2}$$

$$\frac{dT^V}{dz} = \Omega\left(\frac{aJ_e - a\left(J_1\bar{h}_1^V + J_2\bar{h}_2^V\right)}{\left(V_1+V_2\right)c_p^V}\right), \tag{3}$$

$$\frac{dT^L}{dz} = \Omega\left(\frac{-a^H J_q + aJ_e - a\left(J_1\bar{h}_1^L + J_2\bar{h}_2^L\right)}{\left(L_1+L_2\right)c_p^L}\right). \tag{4}$$

The first two equations represent the conservation of mass for each component in the vapor and liquid phases, while the last two are the energy balance equations for each phase. Here, V_k and L_k are the molar flows of component k in the vapor and liquid phases, J_k is the molar flux of component k, J_e is the total energy flux, J_q is the heat flux exchanged with the utility, $\bar{h}_k^\alpha$ and c_p^α are the partial molar enthalpy of

This is the accepted version of an article published in Chemical Engineering Science
http://dx.doi.org/doi.org/10.1016/j.ces.2020.115539

component k and heat capacity of phase α, a is the contact area between the liquid and vapor per unit volume, a^H is the heat exchange area with the utility per unit volume, Ω is the column's cross-section and z is the position (height) in the column.

We introduce the measurable heat flux in the vapor, $J_q'^{,V} = J_e - \left(J_1 \bar{h}_1^V + J_2 \bar{h}_2^V\right)$ and use a different variable to represent the position along the column, $A = za\Omega$. This allows us to reformulate the equations in a more suitable form:

$$\frac{dV_k}{dA} = J_k, \tag{5}$$

$$\frac{dL_k}{dA} = J_k, \tag{6}$$

$$\frac{dT^V}{dA} = \frac{J_q'^{,V}}{Vc_p^V}, \tag{7}$$

$$\frac{dT^L}{dA} = \frac{-\beta J_q + J_q'^{,V} + \left(J_1\left(\bar{h}_1^V - \bar{h}_1^L\right) + J_2\left(\bar{h}_2^V - \bar{h}_2^L\right)\right)}{Lc_p^L}, \tag{8}$$

with $\beta = a^H/a$ and the introduction of the total molar flows of vapor and liquid, V and L.

2.2. Calculation of thermodynamic properties

We used the Peng-Robinson equation of state to calculate thermodynamic departure functions and phase equilibria. The predictions from the model were compared to experimental data for the oxygen-nitrogen mixture. The analysis showed that there was a maximum 5 % error in the calculation of molar enthalpy and heat capacity, and around 1 % error in bubble pressure and vapor composition for the conditions considered. The components' critical properties, acentric factors and ideal gas heat capacities were taken from Perry and Green [18].

2.3. Constitutive equations

In the rate-based, nonequilibrium model, we used the formulation proposed by Taylor and Krishna [29] for the calculation of the molar fluxes and the total energy flux across the interface. It is based on the assumption that the interface resistances are negligible. The vapor and liquid compositions at either side of the interface then correspond to their equilibrium values. The equations for a binary system are [29],

$$c_t^V k^V \left(y_1^V - y_1^I\right) + y_1^V \left(J_1 + J_2\right) - J_1 = 0, \tag{9}$$

$$c_t^L k^L \left(x_1^I - x_1^L\right) + x_1^L \left(J_1 + J_2\right) - J_1 = 0, \tag{10}$$

$$J_q'^{,V} - J_q'^{,L} + \sum_{i=1}^{2} J_i \left(\bar{h}_i^V - \bar{h}_i^L\right) = 0, \tag{11}$$

$$K_1 x_1^I - y_1^I = 0, \tag{12}$$

$$K_2 x_2^I - y_2^I = 0, \tag{13}$$

$$x_1^I + x_2^I - 1 = 0, \tag{14}$$

$$y_1^I + y_2^I - 1 = 0. \tag{15}$$

The first and second equations give the fluxes in the vapor and liquid phases as the sum of a diffusive term, $c_t^V k^V \left(y_1^V - y_1^I\right)$, and a convective term, $y_1^V \left(J_1 + J_2\right)$. The third equation expresses energy conservation at the interface, while the fourth and fifth give the equilibrium conditions (via the K-factors, which must be calculated at the interface temperature, T^I and with the liquid and vapor fractions, x_k^I and y_k^I) at that same point. Finally, the last two equations state that the mole fractions at the interface must sum to unity. We

This is the accepted version of an article published in Chemical Engineering Science
http://dx.doi.org/doi.org/10.1016/j.ces.2020.115539

use c_t^α and k^α for the molar density and mass transfer coefficient in phase α, respectively. The measurable heat fluxes in the vapor and liquid are given by the expressions,

$$J_q'^{,V} = \Lambda^V \left(T^I - T^V\right), \tag{16}$$

$$J_q'^{,L} = \Lambda^L \left(T^I - T^L\right), \tag{17}$$

where Λ^α is the heat transfer coefficient in phase α. In this model, the coupling between the heat and mass fluxes has been neglected. Studies by van der Ham [33] have shown that coupling and interface resistances can affect the values of the fluxes significantly. This should be further explored in future work. For the heat flux within the utility, we used an overall heat transfer coefficient,

$$J_q = U \left(T_\infty - T^L\right), \tag{18}$$

denoting by T_∞ the utility's temperature. The values for the heat and mass transfer coefficients were assumed to be constant in the range considered. We used average values provided by van der Ham [33], assuming the same values of the vapor and liquid films' thickness. For U, we also used the same values as van der Ham [31].

2.4. Boundary conditions

Since the feed introduces a discontinuity in the temperature and molar flow profiles, it is necessary to divide the column model into two different regions (rectification and stripping sections) and provide the appropriate boundary conditions to connect the regions where the feed is introduced. This location is at $z = 0$, with the rectification section spanning from $z = 0^+$ to $z = \ell_R$, and the stripping section spanning from $z = -\ell_S$ to $z = 0^-$. The solutions at $z = 0^+$ and $z = 0^-$ must satisfy the mass and energy balances

$$V_k\left(z = 0^+\right) - V_k\left(z = 0^-\right) - \phi F_k = 0, \tag{19}$$

$$L_k\left(z = 0^+\right) - L_k\left(z = 0^-\right) + (1 - \phi) F_k = 0, \tag{20}$$

$$V\left(z = 0^+\right) h^V - V\left(z = 0^-\right) h^V - \phi F h_F^V = 0, \tag{21}$$

$$L\left(z = 0^+\right) h^L - L\left(z = 0^-\right) h^L + (1 - \phi) F h_F^L = 0. \tag{22}$$

In the above equations, F_k is the component molar flow in the feed, ϕ is the vapor fraction of the feed stream and h^α is the molar enthalpy of phase α, evaluated at the corresponding temperature and composition.

At the top of the rectification section, there is a condenser. The temperature of the reflux is assumed to correspond to the bubble temperature of the mixture and, if we specify the reflux ratio, r, we have that

$$T^L\left(z = \ell_R\right) - T_B = 0, \tag{23}$$

$$r V_k\left(z = \ell_R\right) - (r + 1) L_k\left(z = \ell_R\right) = 0, \tag{24}$$

where T_B is the bubble temperature at the condenser pressure and composition of the reflux. A bubble point calculation has to be performed when solving these boundary conditions.

Since we consider the reboiler to be an ideal equilibrium-stage, the vapor temperature corresponds to the dew point value, T_D. This further provides the composition of the liquid, $x_k^\star$, in equilibrium with the vapor. If the bottoms flow rate, B, is given, then the following conditions must be satisfied:

$$T^V\left(z = -\ell_S\right) - T_D = 0, \tag{25}$$

$$V_k\left(z = -\ell_S\right) + B x_k^\star - L_k\left(z = -\ell_S\right) = 0. \tag{26}$$

This is the accepted version of an article published in Chemical Engineering Science
http://dx.doi.org/doi.org/10.1016/j.ces.2020.115539

2.5. The entropy production

The entropy balance is important since it allows us to not only calculate the entropy production rate, but also perform a consistency check of the model. The total entropy production of the column has contributions from the condenser, rectification section, feed, stripping section and reboiler [11],

$$\frac{dS^{irr}}{dt} = \frac{dS_C^{irr}}{dt} + \frac{dS_{RS}^{irr}}{dt} + \frac{dS_F^{irr}}{dt} + \frac{dS_{SS}^{irr}}{dt} + \frac{dS_R^{irr}}{dt}. \tag{27}$$

The entropy production in the condenser, reboiler and feed are calculated by a macroscopic entropy balance,

$$\frac{dS_C^{irr}}{dt} = Ds^D + L\left(z=\ell_R\right)s^L - V\left(z=\ell_R\right)s^V - \frac{\dot{Q}_C}{T_{C,\infty}}, \tag{28}$$

$$\frac{dS_R^{irr}}{dt} = Bs^B + V\left(z=-\ell_S\right)s^V - L\left(z=-\ell_S\right)s^L - \frac{\dot{Q}_R}{T_{R,\infty}}, \tag{29}$$

$$\frac{dS_F^{irr}}{dt} = V\left(z=0^+\right)s^V - V\left(z=0^-\right)s^V - L\left(z=0^+\right)s^L + L\left(z=0^-\right)s^L - Fs^F. \tag{30}$$

In the above equations, $\dot{Q}_C$ and $\dot{Q}_R$ are the condenser and reboiler duties (which are calculated by means of the energy balance in the equipment), while $T_{C,\infty}$ and $T_{R,\infty}$ are the temperatures of the cold and hot utilities in the condenser and reboiler, respectively. We use s for the molar entropy of the stream, evaluated at the corresponding temperature and composition.

For the rectification and stripping sections, we will use nonequilibrium thermodynamics to compute dS^{irr}/dt. The entropy production is the sum of the products of thermodynamic forces, X_k, and fluxes [13]. In this example, there are four different fluxes; the nitrogen and oxygen molar fluxes, J_1 and J_2, the total energy flux between the liquid and vapor, J_e, and the heat flux between the utility and the liquid, J_q. It is convenient to use the measurable heat flux, J_q', instead of the total heat flux. However, we emphasize that the measurable heat flux is different in the vapor and liquid phases, since the partial molar enthalpies of the components in each phase are unequal. We can select one of the measurable heat fluxes and evaluate the driving forces at the other phase's temperature. In this work, we choose the measurable heat flux of the vapor phase and, then, the chemical potential differences must be evaluated at the liquid temperature [13, 31]. For the molar fluxes we have,

$$X_k = -\frac{1}{T^L}\Delta_{LV}\mu_{k,T} = R\ln\left(\frac{x_k\hat{\phi}_k^L\left(T=T^L\right)}{y_k\hat{\phi}_k^V\left(T=T^L\right)}\right), \tag{31}$$

where $\hat{\phi}_k^\alpha$ are the fugacity coefficients of component k in phase α and Δ_{LV} is the difference in the property between the liquid and vapor phases. They must be evaluated at the liquid temperature. For the thermal driving forces, we have that [31]

$$X_q^{LV} = \Delta_{LV}\frac{1}{T} = \frac{1}{T^V} - \frac{1}{T^L}, \tag{32}$$

$$X_q^{LU} = \Delta_{LU}\frac{1}{T} = \frac{1}{T^L} - \frac{1}{T_S^U}. \tag{33}$$

The local entropy production (per unit area) at any point in section S (which can be either the rectifying or stripping sections), σ_S, is

$$\sigma_S = -J_1\frac{1}{T^L}\Delta_{LV}\mu_{1,T} - J_2\frac{1}{T^L}\Delta_{LV}\mu_{2,T} + J_q'^{,V}\Delta_{LV}\frac{1}{T} + J_q\Delta_{LU}\frac{1}{T}. \tag{34}$$

The total entropy production in the corresponding section can be evaluated by integrating the local entropy source over the total area of the section, A_S,

$$\frac{dS_S^{irr}}{dt} = \int_{A_S}\sigma_S dA. \tag{35}$$

This is the accepted version of an article published in Chemical Engineering Science
http://dx.doi.org/doi.org/10.1016/j.ces.2020.115539

A check of thermodynamic consistency can be performed by comparing the total entropy production from Eq. 27 with that from an overall macroscopic entropy balance [13],

$$\frac{dS^{irr}}{dt} = Ds^D + Bs^B - Fs^F - \frac{\dot{Q}_C}{T_{C,\infty}} - \frac{\dot{Q}_R}{T_{R,\infty}} - \int_A \frac{J_q}{T_\infty} dA. \tag{36}$$

The above equations show that if we constrain the inlet and outlet streams, the only way to influence the entropy production is by changing the heat duties, or exchanging heat at more convenient temperatures. Moreover, the overall energy balance must also be satisfied:

$$Dh^D + Bh^B - Fh^F = \dot{Q}_C + \dot{Q}_R + \int_A J_q dA, \tag{37}$$

with the heat flux calculated with equation 18.

2.6. Reference configuration

The operating conditions of the reference case are based on the work by van der Ham [31] for a low pressure distillation column for air separation. The reference configuration is an adiabatic packed distillation column, where a mixture of nitrogen and oxygen ($y_1 = 0.79$), at 85 K and 0.14 MPa, is fed at a rate of 10.00 mol $\cdot$ s^{-1}. The total exchange area between liquid and vapor is 141 m^2 and 225 m^2 for the rectification and stripping sections, respectively.

The column's bottoms flow rate is 2.05 mol $\cdot$ s^{-1} and the reflux ratio is 2.00. The condenser's utility temperature is 10 K below the distillate's and the reboiler's utility, 20 K above the bottoms. With these operating conditions, the mole fraction of nitrogen in the distillate is 0.985.

3. The numerical procedures

3.1. Solution method

The two-region boundary value problem given by Eqs. 5 to 8, together with the boundary conditions in Eqs. 19 to 26 were solved with MATLAB's function bvp4c, which uses an orthogonal collocation method. The tolerance of the solver was set to an absolute error of 10^{-3}. First, a uniform solution was used on a small part of the column to obtain an initial guess. The solution was next extended to larger spatial intervals and used as an initial guess for a new solution until the interval matched $[-\ell_S, \ell_R]$.

Calculation of the fluxes has be performed at each point in the solution of the constitutive equations, Eq. 9 to 17. One can reduce the complexity of the problem by substituting Eqs. 16 and 17 in 11, which gives only 7 unknowns, J_k, T^I, x_k^I, y_k^I, for which it is easier to estimate initial values. Because of the non-linearity of the system of equations, we used MATLAB's function fsolve, using the initial guesses proposed by Taylor and Krishna [29].

3.2. Minimization of the entropy production

In the optimization, the stripping and rectifying sections exchange heat at every position, z, with a utility that can have any temperature, $T_\infty(z)$. The control variable, $T_\infty(z)$, and reflux ratio are adjusted such that the total entropy production (given by Eq. 36) is minimal. The variables describing the state of the column, molar flows and temperatures of each phase, change so that the conservation equations (Eqs. 5 to 8) are satisfied at each point. For the optimization to be meaningful, constraints need to be imposed. The following parameters were therefore set to be the same as in the reference case:

- The geometrical aspects of the column (diameter, height of packing of rectification and stripping sections, etc).
- The operating pressure.
- The inlet conditions.

This is the accepted version of an article published in Chemical Engineering Science
http://dx.doi.org/doi.org/10.1016/j.ces.2020.115539

- The distillate and bottoms' component molar flows.
- The reboiler and condenser utilities' temperatures.

Fixing the distillate and bottoms' component molar flows determines their temperatures, since they are saturated liquids. This means that in the entropy balance in Eq. 36, the first three terms on the right hand side are given, and any change in the entropy production comes from the heat exchanged. Moreover, due to the overall energy balance, Eq. 37, the sum of the heat duties must be constant (as the left hand side of it is constant).

As variables, we selected the component molar flows, temperatures, the utilities' temperatures and the reflux ratio. The latter plays an important role, as it is related to the heat duty in the condenser. All variables involved are non-negative and were varied within a certain range. For the molar flows, the upper bound was given by 3 times the maximum molar flow; the vapor and liquid temperatures, between 75 K and 100 K, while for the utility, between 70 K and 100 K.

In order to solve the optimization problem, the column section was gridded into N points and we solved a discrete version of the problem (involving a total of $7N + 1$ variables). The differential equations (eqs. 5 to 8) were thus discretized and the resulting algebraic system of equations was used as constraints, together with those specifying the distillate and bottoms' conditions. We used MATLAB's function fmincon, using a sequential quadratic programming solver. In order to aid the solution process, we first used coarse grids (consisting of 16 points) to obtain approximate values of the variables, which we then took as initial guesses for finer grids, using up to 90 points.

4. Results and discussion

4.1. The reference case

Figure 2 shows the component molar flows along the distillation column for the reference configuration. As expected, the molar flow of nitrogen increases continuously from the bottom to the top, while the oxygen molar flow decreases. There is a discontinuity in the profiles at $z = 0$ m, corresponding to the feed stage. Just below $z = 0$, the variation of the molar flows is small, indicating that the molar fluxes are low. This can be explained by Fig. 3, which shows the composition of the different phases at each point in the column. We observe that the vapor interface composition is closer to the vapor mole fraction near the feed stage, which leads to smaller driving forces and fluxes. This effect is not present in a model that assumes equilibrium between vapor and liquid at the outlet of each stage. In the rectification and bottom part of the stripping section, the difference between the corresponding compositions is larger and so are the molar fluxes. Most of the resistance to mass transfer is in the vapor film, since the liquid and interface compositions (on the liquid side) are nearly identical in Fig. 3.

Fig. 4 displays the temperatures through the column for the reference configuration. The liquid and interface temperatures are very similar, which means that most of the resistance to heat transfer is also located at the vapor side of the interface. Similar to Fig. 2, a discontinuity can be seen at the feed location. Even though the liquid and vapor temperatures become closer, there is a temperature gap between them throughout most of the column that comes from the finite-sized heat transfer coefficient.

The reference configuration has a total entropy production of 479 $\mathrm{W \cdot K^{-1}}$. The entropy production was calculated using Eq. 27 with 100 points for the column sections. It was found to be equal to the value given by the overall entropy balance in Eq. 36 within the accuracy of the computations. Together with a careful inspection of the overall energy and mass balances for different parts of the column, this served as a check of a consistent and correct implementation of the model.

Nearly 80% of the entropy is generated in the auxiliary heat transfer equipment. The contributions from the condenser and reboiler are 233 $\mathrm{W \cdot K^{-1}}$ and 146 $\mathrm{W \cdot K^{-1}}$, respectively. The local entropy production profile inside the column is displayed in Fig. 5. Here, the largest entropy production is located near the bottom of the column, whereas there is a large section below the feed where the entropy production is small. This can be explained from the small driving forces and fluxes in this part of the column. The transfer of

This is the accepted version of an article published in Chemical Engineering Science
http://dx.doi.org/doi.org/10.1016/j.ces.2020.115539

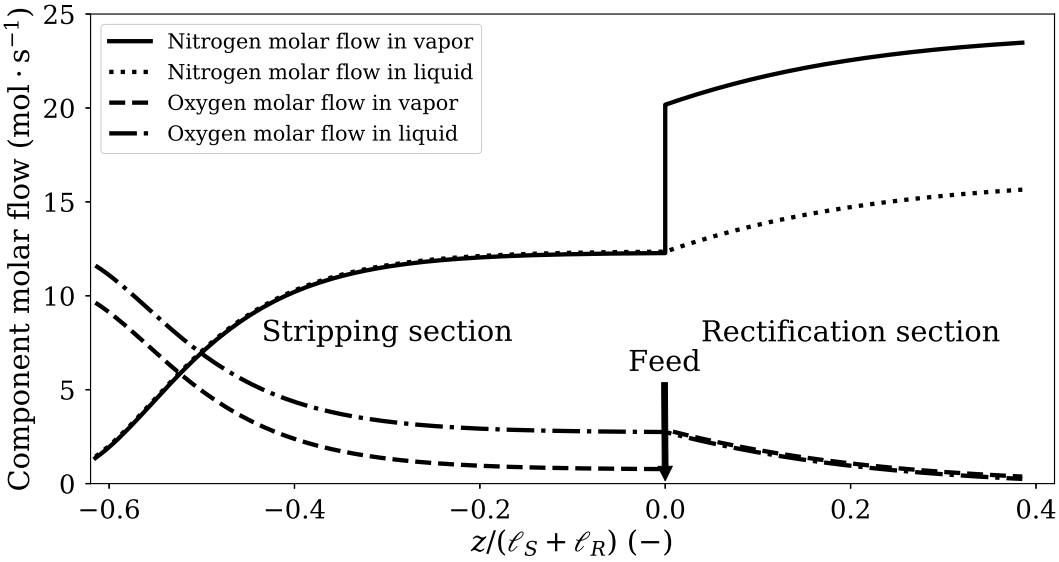

Figure 2: Component molar flows in each phase as a function of the position along the column for the reference configuration.

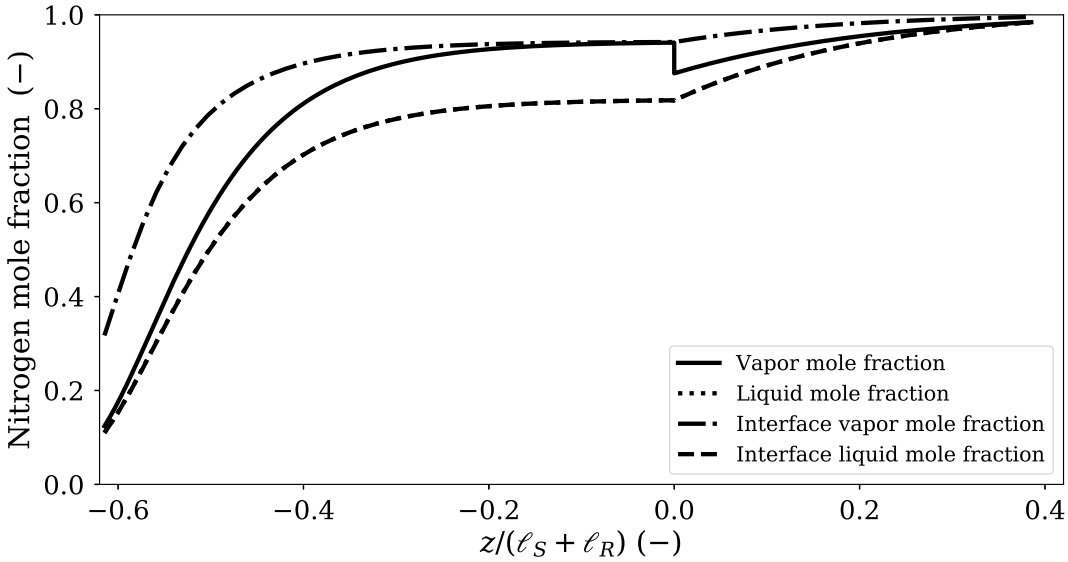

Figure 3: Nitrogen vapor, liquid and interface composition as a function of the position along the column for the reference configuration.

oxygen is responsible for the largest part of the entropy production, followed by the transfer of nitrogen. The heat transfer between liquid and vapor gives a minor contribution to the total entropy production.

To understand the local entropy production, it is helpful to examine how the component molar flows and phase temperatures vary along the column, as displayed in Figs. 2 and 4. Below the feed stage, the molar fluxes are small due to the vapor and interface compositions being close. The corresponding driving force is, accordingly, small and the entropy production is low. A similar reasoning applies to the bottom, where

This is the accepted version of an article published in Chemical Engineering Science
http://dx.doi.org/doi.org/10.1016/j.ces.2020.115539

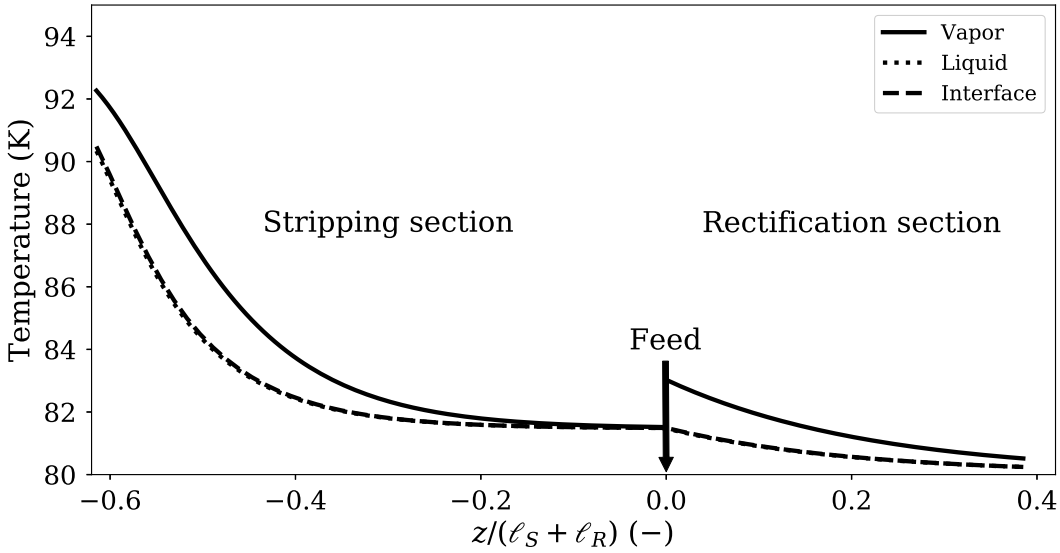

Figure 4: Temperature of each phase and interface as a function of the position along the column for the reference configuration.

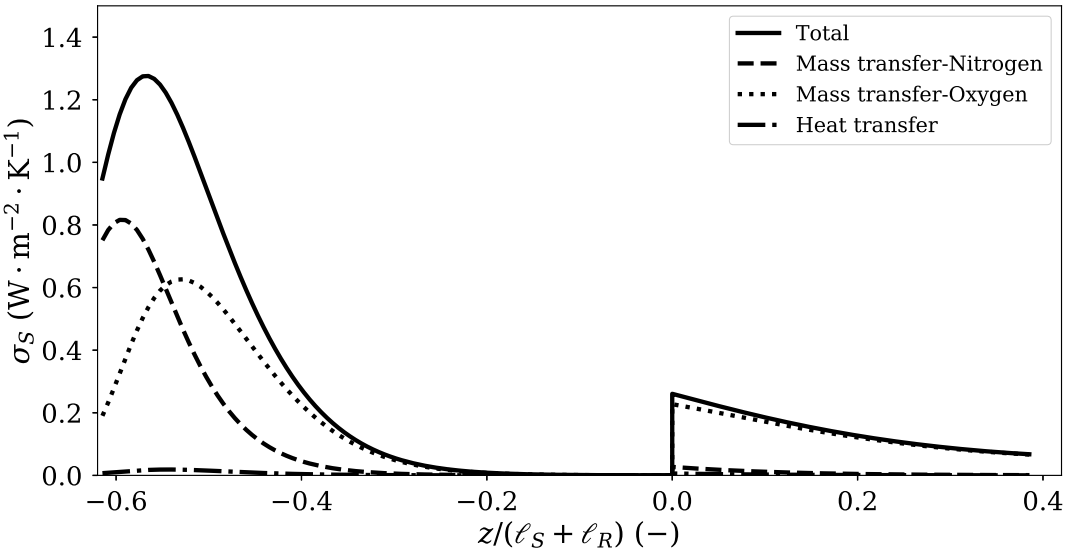

Figure 5: Local entropy production as a function of the position along the column for the reference configuration.

there are larger fluxes and driving forces, which lead to a higher entropy production.

4.2. Diabatic columns with minimum entropy production

The mass transfer rates depend on the conditions at the interface, which are influenced by the states of the bulk phases. Changing the liquid and vapor's temperatures thus allows the mass fluxes to be controlled indirectly. This creates a potential to reduce the total entropy production.

This is the accepted version of an article published in Chemical Engineering Science
http://dx.doi.org/doi.org/10.1016/j.ces.2020.115539

We compare first the results from the reference configuration with a diabatic column that has $\beta U = 8\ \mathrm{W \cdot m^{-2} \cdot K^{-1}}$. A larger number for βU means that more heat transfer area is available, or that the utility has a larger overall heat transfer coefficient (see Eq. 18). Table 1 compares the entropy production of the two configurations. The optimal diabatic configuration decreases the total entropy production by nearly 50 %. A reduction is apparent in all parts of the equipment, except in the rectification section, where there is a slight increase. This is in contrast to the results by Røsjorde and Kjelstrup [22] and Sauar et at. [24], where the equilibrium-stage model was used. Albeit their works examined different binary mixtures, the decrease in the total entropy production came at the expense of a higher entropy production in the column section.

Part	Reference configuration	Optimal diabatic configuration
Condenser	233	151
Rectification section	20	26
Feed	5	1
Stripping section	75	37
Reboiler	146	30
Total	479	245

Table 1: Total entropy production ($\mathrm{W \cdot K^{-1}}$) in each part of the distillation column, for the reference and optimal diabatic ($\beta U = 8\ \mathrm{W \cdot m^{-2} \cdot K^{-1}}$) configurations.

In Tab. 2 we present the total heat exchanged in each part of the column, together with the net heating and cooling duties for the reference and optimal diabatic configurations (with $\beta U = 8\ \mathrm{W \cdot m^{-2} \cdot K^{-1}}$). We find that by operating the column optimally, the net heating and cooling are both reduced by 37 kW, i.e. by nearly 50% and 30% respectively. Moreover, the heat can be delivered at lower temperatures and withdrawn at higher temperatures than in the reference configuration.

Part	Reference configuration	Optimal diabatic configuration
Condenser	-130	-84
Rectification section	0	-9
Stripping section	0	20
Reboiler	72	15
Net cooling	-130	-93
Net heating	72	35

Table 2: Heat exchanged in the different parts of the column (kW), for the reference and optimal diabatic configurations with $\beta U = 8\ \mathrm{W \cdot m^{-2} \cdot K^{-1}}$.

The fact that the total heating/cooling duties and the total entropy production are all reduced, differs from previous works that used the equilibrium-stage model, e.g. by Johannessen and Røsjorde [11] and Røsjorde and Kjelstrup [22]. In their optimizations, the entropy production was reduced, but at the expense of larger heating/cooling duties. In Sec. 4.3, we will discuss whether this is also the case for the example investigated in this work. A key limitation of the equilibrium-stage model is that the distribution of components is determined by the equilibrium condition. In a non-equilibrium model, the components distribute according to their mass transfer rates, which can be controlled up to some point by allowing for heat exchange.

Fig. 6 shows that heat goes out of the column in the rectifying section, while heat enters the column in the stripping section. A major advantage of the diabatic configuration is that the vapor and liquid molar flows are reduced, as a result of the decrease in the operating reflux ratio. The molar flows inside the column for the reference and optimal diabatic configurations are compared in figure 7.

Figure 8 shows the local entropy production inside the column for the optimal diabatic configuration. In contrast to Fig. 5, the entropy production is more evenly distributed throughout the column. The largest contribution in the optimal configuration comes from heat transfer with the utility; transfer of nitrogen is responsible for a large part of the generation at the bottom of the column, while oxygen transfer gives a

This is the accepted version of an article published in Chemical Engineering Science
http://dx.doi.org/doi.org/10.1016/j.ces.2020.115539

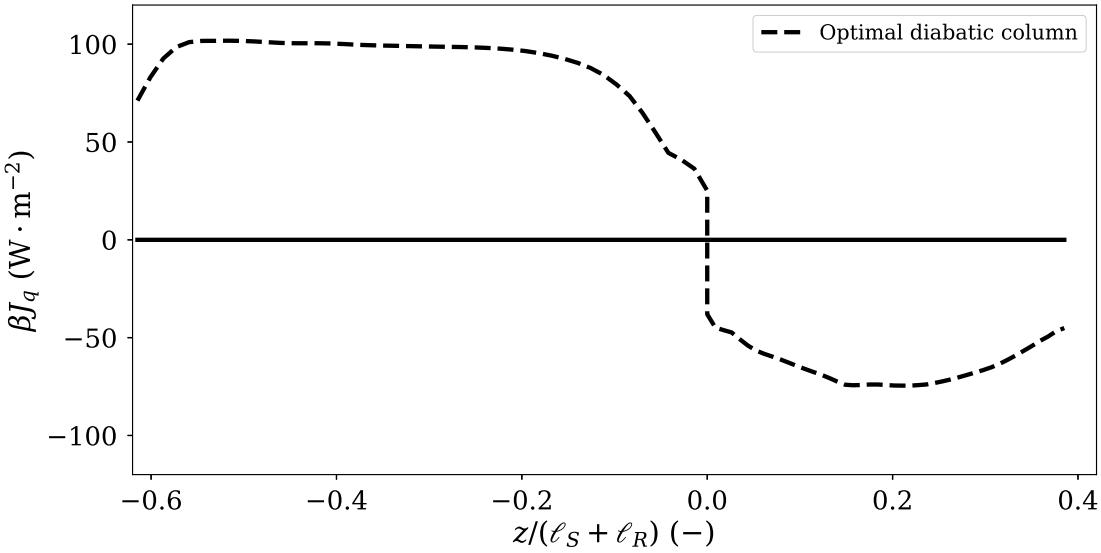

Figure 6: Heat flux (W · m^{-2}) exchanged with the utility as a function of the position along the column for the optimal diabatic configuration with $\beta U = 8$ W · m^{-2} · K^{-1}.

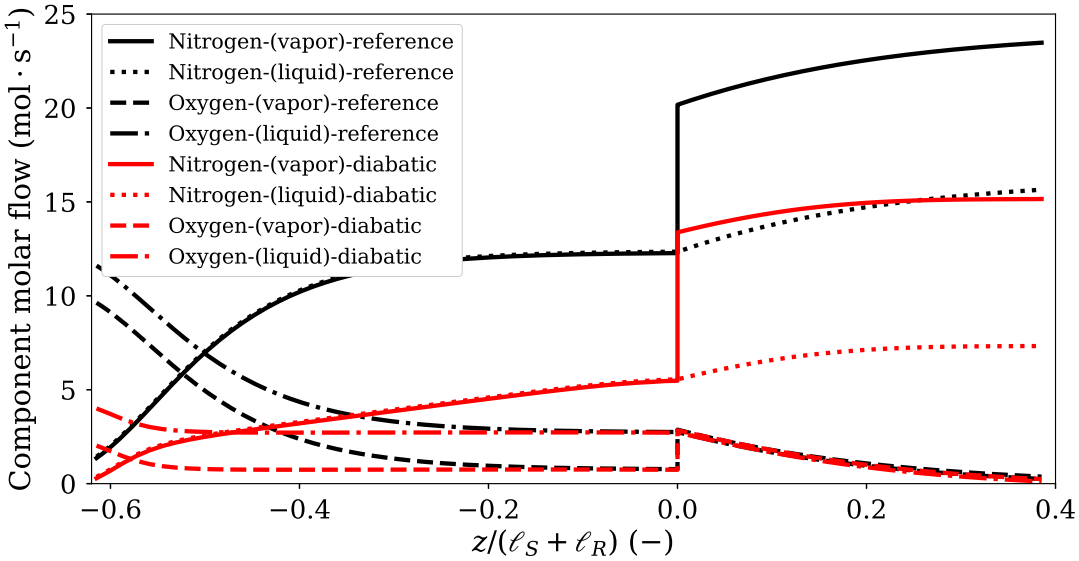

Figure 7: Component molar flows (mol · s^{-1}) in each phase as a function of the position along the column for the optimal diabatic configuration ($\beta U = 8$ W · m^{-2} · K^{-1}) and reference configuration.

larger contribution in the rectification section.

The change in the local entropy production in the optimal case can be understood by comparing the temperature (figure 9) and composition profiles along the column (figure 10). In the optimal diabatic configuration, the temperature gap between the vapor and liquid is smaller than in the reference configuration. This leads to a decrease in the entropy production from heat exchange between the phases, which was

This is the accepted version of an article published in Chemical Engineering Science
http://dx.doi.org/doi.org/10.1016/j.ces.2020.115539

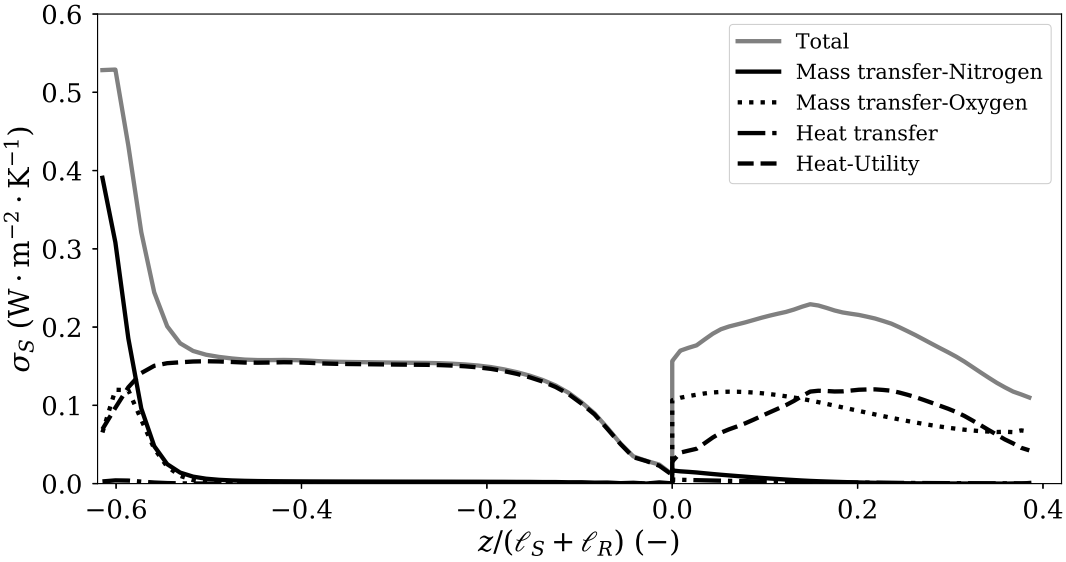

Figure 8: Local entropy production as a function of the position along the column for the optimal diabatic configuration for $\beta U = 8$ W · m^{-2} · K^{-1}.

already small in the reference configuration. A closer inspection of the vapor composition shows that it is generally closer to the equilibrium line[1] in the diabatic configuration. Hence, the driving forces for mass transfer and the corresponding fluxes are smaller, leading to a lower entropy production. The difference between the vapor and equilibrium concentrations is larger near the bottom, while it is almost negligible near the feed stage. This explains the shape of the entropy production curve in the stripping section in Fig. 8.

In the optimal case, the driving forces for mass transport are also smaller because there is less mass of each component to transfer from one phase to the other. This is a consequence of the reduction of the molar flow rates in the column due to the decrease of the reflux ratio. The composition of the liquid in the lowest point is closer to the bottoms' mole fraction. This means that the fraction of liquid that is vaporized in the reboiler is smaller. As the molar flows are also smaller, the entropy production in the reboiler is reduced.

Fig. 11 shows the local entropy production in the rectification and stripping sections for optimal diabatic configurations with different values of βU. When the value of βU becomes larger, the local entropy production becomes more uniformly distributed in space and the total entropy production decreases (as can be seen from Tab. 3). This is in agreement with the hypothesis put forward by Johannessen and coworkers [10, 11], that the system will have more freedom to adapt as the heat exchange area (in our case, the product of the exchange area and U) becomes larger. As the system has more freedom, it will, according to the hypothesis, approach equipartition of the entropy production. Equipartition of the entropy production is not fulfilled in a strict mathematical sense, but it is still a good approximation to the state of minimum entropy production. Fig. 10 shows that as βU becomes larger, the vapor composition moves closer to the equilibrium line, which leads to a lower entropy production and a reduction in the boil up ratio.

The total heat heating (and cooling) duties are also reduced for the optimal diabatic configurations (see Tab. 3). The largest reduction in heat duty is in the reboiler, where the temperature difference is large (20 K). Moreover, the operating curve in the $x - y$ diagram (Fig. 10) lies closer to the equilibrium line.

[1]Since mass transfer is controlled by the vapor phase, the composition on the liquid side at the interface is practically the same as in the bulk liquid. Therefore, the vapor equilibrium line gives a good approximation of the vapor interface composition, since the liquid, vapor and interface temperatures are very close.

This is the accepted version of an article published in Chemical Engineering Science
http://dx.doi.org/doi.org/10.1016/j.ces.2020.115539

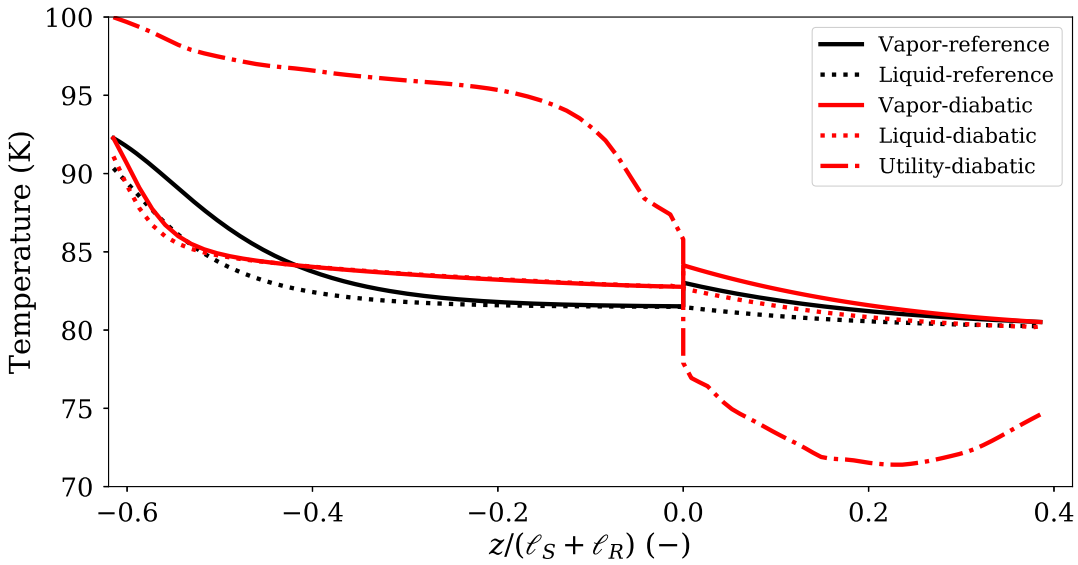

Figure 9: Temperature for the utility, vapor and liquid phases as a function of the position along the column for the optimal diabatic ($\beta U = 8\ \mathrm{W \cdot m^{-2} \cdot K^{-1}}$) and reference configurations.

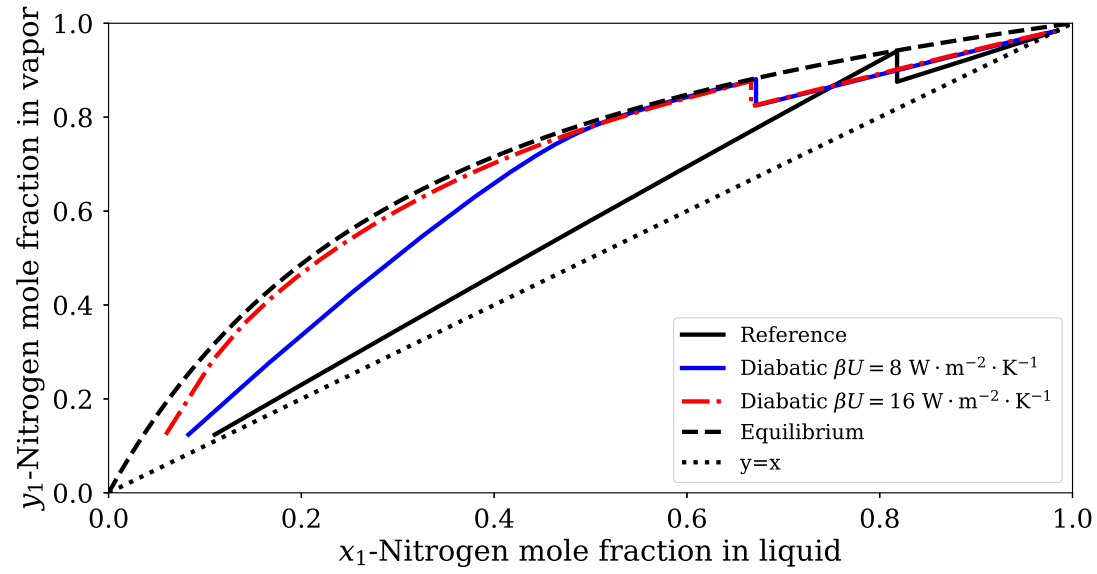

Figure 10: Vapor phase composition as a function of the liquid phase composition for the optimal diabatic ($\beta U = 8\ \mathrm{W \cdot m^{-2} \cdot K^{-1}}$ and $\beta U = 16\ \mathrm{W \cdot m^{-2} \cdot K^{-1}}$) and reference configurations.

This results in a smaller fraction of the liquid being vaporized in the reboiler and, since the molar flows are smaller, the duty is reduced.

This is the accepted version of an article published in Chemical Engineering Science
http://dx.doi.org/doi.org/10.1016/j.ces.2020.115539

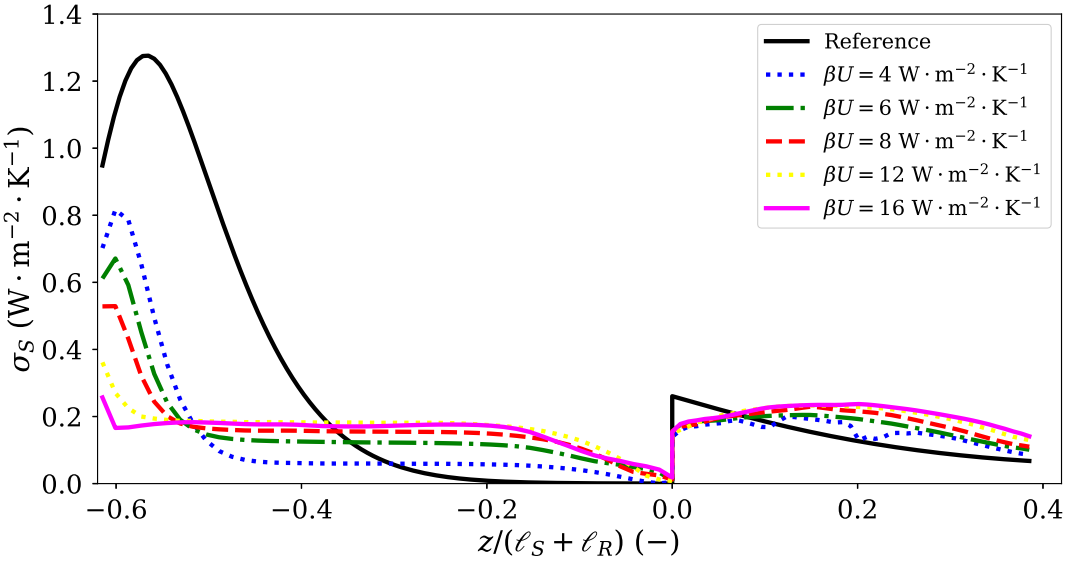

Figure 11: Local entropy production as a function of the position along the column for the reference case and optimal diabatic configurations, using different values of βU.

βU ($\mathrm{W \cdot m^{-2} \cdot K^{-1}}$)	Reference	4	6	8	12	16
$\dot{Q}_C$ (kW)	-130	-89	-86	-84	-80	-78
$\dot{Q}_R$ (kW)	72	28	20	15	8	5
Net cooling (kW)	-130	-94	-94	-93	-93	-93
Net heating (kW)	72	36	36	35	35	35
dS^{irr}/dt ($\mathrm{W \cdot K^{-1}}$)	479	267	255	245	227	214

Table 3: Heat exchanged in the column, reboiler and condenser (kW) and entropy production ($\mathrm{W \cdot K^{-1}}$) for the reference and optimal diabatic configurations for different values of βU.

4.3. Comparison of the state of minimum entropy production in equilibrium-stage and rate-based models

We shall next compare the rate-based column model to the equilibrium-stage model. Since the equilibrium-stage model has been extensively documented in the literature, we refer the reader to previous works for further details [11, 27]. In particular, we will investigate whether a decrease in the entropy production in the equilibrium-stage model comes at the expense of a larger heating/cooling duty, similar to previous examples in the literature [11, 22, 24]. To that end, we performed an entropy generation minimization of a diabatic distillation column using the equilibrium-stage model. The number of trays was 6, which gave a nitrogen mole fraction in the distillate of 0.984, similar to the one from the non-equilibrium model. All other variables (feed, distillate rate, reflux ratio) were set to the same values as in the reference case. The results are presented in Tab. 4, where different values of UA^H have been examined, i.e. the product of the heat transfer coefficient and total tray heat exchange area.

The entropy production is reduced, but not as much as in the non-equilibrium model. The most striking difference lies in the overall heating and cooling duties. While the rate-based model gives a reduction in the heating/cooling duties (see Tab. 3), the equilibrium rate model gives an increase in the cooling/heating duties as the total entropy production decreases. This is the same trend as in the works of Johannessen and Røsjorde [11, 21] and Sauar et al. [24]. We hypothesize that this must be an inherent limitation of the equilibrium-stage model.

This is the accepted version of an article published in Chemical Engineering Science
http://dx.doi.org/doi.org/10.1016/j.ces.2020.115539

UA^H ($\mathrm{W \cdot K^{-1}}$)	Reference	800	1200	3000	5000
$\dot{Q}_C$ (kW)	-130	-129	-121	-106	-93
$\dot{Q}_R$ (kW)	72	65	63	49	43
Net cooling (kW)	-130	-133	-134	-139	-143
Net heating (kW)	72	75	76	81	85
dS^{irr}/dt ($\mathrm{W \cdot K^{-1}}$)	472	460	451	423	399

Table 4: Heat exchanged in the column, reboiler and condenser (kW) and entropy production ($\mathrm{W \cdot K^{-1}}$) for the reference and optimal diabatic configurations for different values of UA^H, using a 6-tray column with the equilibrium-stage model.

4.4. How to realize energy efficient operation in industrial scale columns

The analysis in the present work was performed with a column that is smaller than the typical industrial scale distillation column. The value of β is inversely proportional to the diameter of the column. Hence, to realize the same βU values for larger columns requires a higher overall heat transfer coefficient or more available heat transfer area.

An attractive possibility is to search for ways to increase the heat transfer area. This can be accomplished by including heating/cooling pipes inside the column, or using specially designed heat exchangers at specified locations in the column. De Koeijer et al. [4] provided a sketch of a diabatic distillation column with different areas allocated to each region. The optimal heat exchange profiles presented in the present paper give a good estimate of the theoretical minimum of the entropy production and serve as a benchmark for air separation.

In terms of practical application, the column can be built with two different annular heat exchanging sections or jackets: one for heating the stripping section and the other for cooling the rectification section. Since the temperature of the utility decreases in an approximately linear fashion in the stripping section, it is possible to calculate the molar flow of a utility exchanging sensible heat. A similar reasoning can be used for the rectifying section. There are, however, some parts where the optimal profile for the utility has the opposite trend, i.e. it increases along the stripping section and decreases in the rectification section. This would require either to use a variable heat exchange area (which may be impractical) or accept this deviation from the optimal configuration. Since the majority of the entropy production is located in the condenser, we can expect that such changes do not alter significantly the total entropy production.

Further improvements can be realized if the heat that is removed in the rectification section can be taken advantage of. This is the case for the HIDiC [17]. A successful commercial implementation of this technology was achieved using four heat exchangers to partially integrate the stripping and rectification sections [34]. An extension of the model presented in this work could be used to evaluate the minimum entropy production of such configurations and of closely integrated distillation columns.

4.5. Energy efficient design and operation

We have observed that the optimal diabatic configuration has a more uniform local entropy production than the reference case. The effect becomes more pronounced as the heat transfer coefficient or exchange area are increased. This serves as another example were equipartition of the entropy production approximates well the state of minimum entropy production. Johannessen and Kjelstrup [9] reported similar findings for chemical reactors and Magnanelli et al. [16], for membrane separation of gases. Another concept that has been recently discussed in the literature is energy efficient highways in state-space [7, 9, 36]. Whether such highways also exists for continuous, rate-based distillation columns remains to be investigated.

4.6. Guidelines for process simulator users

Users of software for process simulations that include design tools for distillation columns can take advantage of several of the findings in this work. Diabatic operation of a distillation column introduces additional degrees of freedom to reduce the reflux ratio, the total entropy production and the heating/cooling duties while maintaining distillate specifications such as molar flow and purity. An important tool to reveal opportunities for increased energy efficiency is a map of the local entropy production along the column. Provided that the product of the area and the overall heat transfer coefficient is sufficiently large, a guideline

This is the accepted version of an article published in Chemical Engineering Science
http://dx.doi.org/doi.org/10.1016/j.ces.2020.115539

for energy efficient design and operation is to approach a uniform distribution of the local entropy production. For distillation columns, such maps serve a similar purpose as the composite curves that are frequently used in heat exchanger design, where a uniform temperature difference is the goal [35].

The work has revealed important differences between rate-based and equilibrium stage models for simulation of diabatic distillation columns. While both the total entropy production and the duties can be reduced in a rate-based model, there is a trade-off in the equilibrium-stage model. This means that the latter model is likely to overestimate the duties in the column. Further experimental work on diabatic columns is required to shed further light on this issue. The reliability of the rate-based model depends on accurate estimates of heat and mass transfer coefficients.

5. Conclusions

In this work, we have presented a distillation column model for separation of air in a low pressure packed distillation column. The model consisted of steady-state balance equations for the condenser, reboiler, mixing in the feed stage, stripping and rectification sections. A nonequilibrium, rate-based formulation was employed, where the temperature and chemical potentials of the gas and liquid-phases were allowed to differ through the column.

We examined in detail a diabatic column that was allowed to heat exchange at each spatial position with a heat utility. The spatial temperature profile of the heat utility was controlled so that the total entropy production in the distillation column was minimized. This resulted in a 50% reduction of the total entropy production. The heating and cooling duties were reduced by 37 kW, representing nearly 30 % and 50 % of the cooling and heating duties respectively.

For the optimal diabatic configurations, the local entropy production in the column sections displayed a more uniform distribution than in the reference case. Moreover, as the heat transfer coefficient was increased, the total entropy production decreased and the local entropy production became more uniform. Hence, the theorem of equipartition of entropy production serves as a good approximation to the state of minimum entropy production.

Results from the rate-based (nonequilibrium) model were compared to those from an equilibrium-stage model. While both the entropy production and the heating/cooling duties were reduced in the rate-based model, the decrease of the total entropy production in the equilibrium-stage model came at the expense of larger heating/cooling duties. We hypothesize that this is a general limitation of equilibrium-stage models. This emphasizes the need for more accurate models, for instance, including coupling effects and interfacial resistances [31], as well as experimental results to provide reliable guidelines on how to optimize the performance of distillation columns in the future.

6. Acknowledgements

Diego Kingston would like to thank Universidad de Buenos Aires for travel grant to visit the Center of Excellence PoreLab, given by Res. C.S. 1561/18. This publication has been partly funded by HighEFF - Centre for an Energy Efficient and Competitive Industry for the Future, an 8 year Research Centre under the FME-scheme (Centre for Environment-friendly Energy Research, 257632). The authors are grateful to the Research Council of Norway for PoreLab Center of Excellence, project no. 262644. The authors are grateful to Eivind Johannessen for valuable comments at the start of this work and making available his code for entropy production minimization to understand programming issues.

References

[1] R. Agrawal and D. W. Woodward, *Efficient cryogenic nitrogen generators: An exergy analysis*, Gas Separation and Purification, 5 (1991), pp. 139–150.

[2] L. Chang and X. Liu, *Non-equilibrium stage based modeling of heat integrated air separation columns*, Separation and Purification Techonology, 134 (2014), pp. 73–81.

[3] G. De Koeijer and R. Rivero, *Entropy production and exergy loss in experimental distillation columns*, Chemical Engineering Science, 58 (2003), pp. 1587–1597.
[4] G. De Koeijer, A. Røsjorde, and S. Kjelstrup, *Distribution of heat exchange in optimum diabatic distillation columns*, Energy, 29 (2004), pp. 2425–2440.
[5] G. M. De Koeijer, S. Kjelstrup, P. Salamon, G. Siragusa, M. Schaller, and K. H. Hoffmann, *Comparison of Entropy Production Rate Minimization Methods for Binary Diabatic Distillation*, Industrial & Engineering Chemistry Research, 41 (2002), pp. 5826–5834.
[6] C. Fu and T. Gundersen, *Using exergy analysis to reduce power consumption in air separation units for oxy-combustion processes*, Energy, 44 (2012), pp. 60–68.
[7] R. Hånde and Ø. Wilhelmsen, *Minimum entropy generation in a heat exchanger in the cryogenic part of the hydrogen liquefaction process: On the validity of equipartition and disappearance of the highway*, International Journal of Hydrogen Energy, 44 (2019), pp. 15045–15055.
[8] E. Johannessen, *The state of minimum entropy production in an optimally controlled system*, PhD thesis, Norges teknisk-naturvitenskapelige universitet, 2004.
[9] E. Johannessen and S. Kjelstrup, *Minimum entropy production rate in plug flow reactors: An optimal control problem solved for SO_2 oxidation*, Energy, 29 (2004), pp. 2403–2423.
[10] ———, *A highway in state space for reactors with minimum entropy production*, Chemical Engineering Science, 60 (2005), pp. 3347–3361.
[11] E. Johannessen and A. Røsjorde, *Equipartition of entropy production as an approximation to the state of minimum entropy production in diabatic distillation*, Energy, 32 (2007), pp. 467–473.
[12] A. A. Kiss and Ž. Olujić, *A review on process intensification in internally heat-integrated distillation columns*, Chemical Engineering and Processing: Process Intensification, 86 (2014), pp. 125–144.
[13] S. Kjelstrup, D. Bedeaux, E. Johannessen, and J. Gross, *Non-Equilibrium Thermodynamics for Engineers*, World Scientific Co., 2nd ed., 2017.
[14] S. Kjelstrup Ratkje, E. Sauar, E. M. Hansen, K. M. Lien, and B. Hafskjold, *Analysis of Entropy Production Rates for Design of Distillation Columns*, Industrial & Engineering Chemistry Research, 34 (1995), pp. 3001–3007.
[15] R. Krishnamurthy and R. Taylor, *A nonequilibrium stage model of multicomponent separation processes. Part II: Comparison with experiment*, AIChE Journal, 31 (1985), pp. 456–465.
[16] E. Magnanelli, Ø. Wilhelmsen, E. Johannessen, and S. Kjelstrup, *Energy efficient design of membrane processes by use of entropy production minimization*, Computers and Chemical Engineering, 117 (2018), pp. 105–116.
[17] M. Nakaiwa, K. Huang, A. Endo, T. Ohmori, T. Akiya, and T. Takamatsu, *Internally heat-integrated distillation columns: A review*, Chemical Engineering Research and Design, 81 (2003), pp. 162–177.
[18] R. H. Perry and D. W. Green, *Perry's Chemical Engineers'Handbook*, McGrawHill, 8th ed., 2008.
[19] R. Rivero, T. Cachot, and P. Le Goff, *Exergy Analysis of Adiabatic and Diabatic Distillation Columns : An Experimental Study*, Energy Efficiency in Process Technology, (1993), pp. 1254–1267.
[20] J. Rizk, M. Nemer, and D. Clodic, *A real column design exergy optimization of a cryogenic air separation unit*, Energy, 37 (2012), pp. 417–429.
[21] A. Røsjorde, *Minimization of entropy production in separate and connected process units*, PhD thesis, Norges teknisk-naturvitenskapelige universitet, 2004.
[22] A. Røsjorde and S. Kjelstrup, *The second law optimal state of a diabatic binary tray distillation column*, Chemical Engineering Science, 60 (2005), pp. 1199–1210.
[23] E. Sauar, R. Rivero, S. Kjelstrup, and K. M. Lien, *Diabatic column optimization compared to isoforce columns*, Energy Conversion and Management, 38 (1997), pp. 1777–1783.
[24] E. Sauar, G. Siragusa, and B. Andresen, *Equal thermodynamic distance and equipartition of forces principles applied to binary distillation*, Journal of Physical Chemistry A, 105 (2001), pp. 2312–2320.
[25] M. Schaller, K. H. Hoffmann, R. Rivero, B. Andresen, and P. Salamon, *The influence of heat transfer irreversibilities on the optimal performance of diabatic distillation columns*, Journal of Non-Equilibrium Thermodynamics, 27 (2002), pp. 257–269.
[26] M. Schaller, K. H. Hoffmann, G. Siragusa, P. Salamon, and B. Andresen, *Numerically optimized performance of diabatic distillation columns*, Computers & Chemical Engineering, 25 (2001), pp. 1537–1548.
[27] J. D. Seader, E. J. Henley, and D. K. Roper, *Separation Process Principles. Chemical and Biochemical Operations*, John Wiley and Sons, Hoboken, NJ, 3rd ed., 2011.
[28] T. Takamatsu, V. Lueprasitsakul, and M. Nakaiwa, *Modeling and design method for internal heat-integrated packed distillation column*, Journal of Chemical Engineering of Japan, 21 (1988), pp. 595–601.
[29] R. Taylor and R. Krishna, *Multicomponent Mass Transfer*, John Wiley & Sons, Ltd., New York, 1992.
[30] D. Tondeur and E. Kvaalen, *Equipartition of entropy production. An optimality criterion for transfer and separation processes*, Industrial and Engineering Chemistry Research, 26 (1987), pp. 50–56.
[31] L. V. van der Ham, *Improving the Second law efficiency of a cryogenic air separation unit*, ph.d. thesis, Norges teknisk-naturvitenskapelige universitet, 2011.
[32] L. V. Van Der Ham, *Improving the exergy efficiency of a cryogenic air separation unit as part of an integrated gasification combined cycle*, Energy Conversion and Management, 61 (2012), pp. 31–42.
[33] L. V. van der Ham, R. Bock, and S. Kjelstrup, *Modelling the coupled transfer of mass and thermal energy in the vapour-liquid region of a nitrogen-oxygen mixture*, Chemical Engineering Science, 65 (2010), pp. 2236–2248.
[34] T. Wakabayashi, K. Yoshitani, H. Takahashi, and S. Hasebe, *Verification of energy conservation for discretely heat integrated distillation column through commercial operation*, Chemical Engineering Research and Design, (2019), pp. 1–12.

This is the accepted version of an article published in Chemical Engineering Science
http://dx.doi.org/doi.org/10.1016/j.ces.2020.115539